FT-IR studies of decarbonylation and recarbonylation of $[Pt_3(CO)_6]_5^{2-}$ supported on dehydrated SiO_2

Junko N. Kondo, Toshiya Yokota, Kazunari Domen [1] and Chiaki Hirose

Research Laboratory of Resources Utilization, Tokyo Institute of Technology, 4259 Nagatsuta, Midori-ku, Yokohama 226, Japan

Received 5 November 1995; accepted 28 March 1996

Decarbonylation of $[Pt_3(CO)_6]_5$ on SiO_2 at 373 K produced $[Pt_3(t\text{-}CO)_3]_5$ species, where all the terminal CO remained. Complete decarbonylation at 423 K was not observed, which led to aggregation at 473 K. The interaction of some Pt with SiO_2 inhibited complete recarbonylation to $[Pt_3(CO)_6]_5$.

Keywords: FT-IR; $[Pt_3(CO)_6]_5^{2-}$

1. Introduction

The nature of a particle or a cluster of a metal varies from that of a single atom to that of a group by increasing the number of constituent atoms. Understanding of the chemistry and function of metal particles will be advanced by investigating the nature of discrete, structurally uniform metal clusters. This has been vigorously attempted by forming highly dispersed metal particles with a known number of atoms on inorganic oxides by thermal decomposition of a supported organometallic compound [1,2]. Fixation of metal carbonyl clusters on oxides with high surface area and their thermal decarbonylation have been examined by infrared (IR) spectroscopy, extended X-ray absorption fine structure (EXAFS), etc. [3–8]. It has been found that a part of the coordinated CO molecules of carbonyl clusters of Os [4], Ru [5], Rh [6] and Ir [7] are desorbed by thermal treatment below 423 K, and that highly dispersed multinuclear metal sites are generated on the oxides [3].

Supported Pt catalysts have been widely used and studied by various methods [9]. Recently, attempts have been made to produce ultra-fine Pt particles on oxide supports by using Pt carbonyl clusters [8,10–12]. A series of Pt carbonyl clusters $[Pt_3(CO)_6]_n^{2-}$ (n = 1 to 6, and 10) [13,14] can be selectively produced by changing the preparation conditions. One unit of $[Pt_3(CO)_6]$ includes a triangular Pt_3 skeleton and three terminal and bridged CO groups, respectively, and the units join with the unit planes parallel with each other by numbers of n. The structure of $[Pt_3(CO)_6]_5$, where $n = 5$, is shown in the inset of fig. 1. The use of these Pt clusters as starting materials to form Pt particles with uniform numbers of atoms on oxides will provide valuable information on the nature of metal particles with small constituent numbers, which would be different from that of metal particles of a few tens Å in size. However, studies on supported Pt catalysts prepared by Pt carbonyl clusters are limited because of their poor stability in the air. In this study, $[Pt_3(CO)_6]_5^{2-}$ was anchored on dehydrated SiO_2, and thermal decarbonylation and recarbonylation by exposure to CO were studied by IR spectroscopy. The nature and the stability of the clusters are discussed.

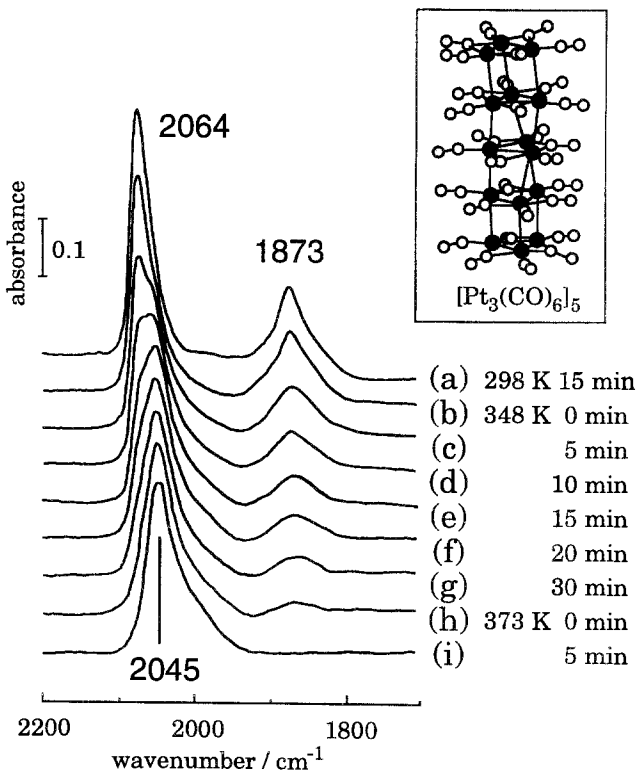

Fig. 1. Thermal treatment of $[Pt_3(CO)_6]_5$ on SiO_2 at 298 K (a), 348 K (b–g) and 373 K (h,i). Spectra were measured soon (b), at 5 min, (c), 10 min (d), 15 min (e), 20 min (f) and 30 min (g) after the temperature of the sample was raised to 348 K, and soon (h) and at 5 min (i) at 373 K. The inset shows the structure of $[Pt_3(CO)_6]_5$, where ⊃–○, –○–○ and ● indicate a t-CO, b-CO and a Pt atom, respectively.

[1] To whom correspondence should be addressed.

2. Experimental

$[Pt_3(CO)_6]_5^{2-}$ was prepared in a Schlenk flask according to the procedure described in ref. [15]. 1.0 g of $Na_2PtCl_6 \cdot nH_2O$ (Kojima Chem. Co. Ltd.) was resolved in 17.5 ml of CH_3OH (Kanto Chem. Co. Ltd.) and reduced by 1.4 g of CH_3COONa (Kosou Chem. Co. Ltd.) under CO (Toyo Sanso Co. Ltd.) atmosphere for 24 h. After confirming the uniform production of $[Pt_3(CO)_6]_5^{2-}$ by an IR spectrum, the solution was filtered and crystallized in 5.0 ml of CH_3OH solution containing 0.5 g of $N(n\text{-}C_4H_9)_4Cl$ (Tokyo Kasei Co. Ltd.). The obtained $[Pt_3(CO)_6]_5^{2-} \cdot [N(n\text{-}C_4H_9)_4]_2^+$ was washed with CH_3OH several times.

A disk (81 mg, 20 mm in diameter) of SiO_2 (Aerosil 300, surface area 300 $m^2\ g^{-1}$) was dehydrated by evacuation at 773 K for 1 h in an IR cell connected to a closed gas circulation system. Then the sample disk was cooled to room temperature under evacuation followed by introducing Ar. 6.7 ml of the THF solution of $[Pt_3(CO)_6]_5^{2-}$ (3.5×10^{-4} mol ℓ^{-1}) was dropped into the pretreated SiO_2 disk in Ar atmosphere, and the solvent was removed by flowing Ar gas in the system. The amount of supported cluster was 0.08 wt% or 1 cluster per 420 $Å^2$, assuming that the loaded cluster dispersed uniformly.

IR spectra were recorded on a Fourier transform (FT) IR with a triglycine sulfate (TGS) detector at 4 cm^{-1} resolution. 16 scans were averaged for one spectrum. All the spectra were obtained after subtracting the background spectra of SiO_2 taken under evacuation at the same temperatures. For recarbonylation and hydrogen treatment, 400 Torr of CO and 100 Torr of H_2 were exposed to the sample.

3. Results and discussion

3.1. Thermal decarbonylation

The change of IR spectra of $[Pt_3(CO)_6]_5^{2-}$ supported on SiO_2 by heating from 298 to 373 K under evacuation is shown in fig. 1. After evacuation at 298 K for 15 min (fig. 1 (a)) two bands were observed at 2064 and 1873 cm^{-1} which are assigned to terminal (t-) and bridged (b-) CO, respectively. By evacuation at 298 K, slight changes in IR spectra between before and after evacuation were observed; the peak of t-CO shifted from 2058 to 2064 cm^{-1} and the full width at half maximum (FWHM) increased from 25 to 35 cm^{-1}. These changes of the IR band of t-CO took place alongside the desorption of THF, which interacted with surface hydroxyl (silanol) groups of the support. The free silanol groups regenerated after desorption of THF may in turn interact with the Pt cluster. The increase in the band width was interpreted in terms of inhomogeneous broadening resulting from various types of interaction of $[Pt_3(CO)_6]_5^{2-}$ with surface silanol groups. The interaction of the cluster with silanol groups is regarded as weak hydrogen bonding because decarbonylation which produces coordination unsaturated Pt atoms did not proceed at this stage. The similar IR spectrum of the cluster on the support after evacuation to that in the solvent denotes that the structure of $[Pt_3(CO)_6]_5^{2-}$ is not much distorted by hydrogen bonding, judging from the spectrum. However, the number of silanol groups interacting with one $[Pt_3(CO)_6]_5^{2-}$ cluster and whether the clusters exist parallel with or perpendicular to the surface are not clear, and their variation is regarded as an origin of the inhomogeneity. At 348 K (fig. 1(b)–(g)) a decrease of the band of b-CO was observed in the time course, and the band due to t-CO shifted to lower frequency. The shift of the t-CO band is unlikely due to dipole–dipole interaction where a band continuously shifts with increasing or decreasing the coverage [15]. It is rather interpreted as follows. The frequency of the t-CO band is centered at 2064 cm^{-1} when b-CO is present. As the b-CO is removed the frequency shifts to 2045 cm^{-1} which is characteristic for t-CO in the absence of b-CO. This shift is brought about by the desorption of bridge-bonded CO. Consequently, an increased back bonding from the b-CO-free Pt atoms to the t-CO molecules is observed that manifests itself as a redshift of the C–O stretching frequency. In other words, the same adsorbed CO species is present in two distinct environments, i.e. in the presence of b-CO (2064 cm^{-1} band) and in the absence of b-CO (2045 cm^{-1} band). The interconversion of t-CO also appeared in the IR spectra observed by Handy et al. [10], who studied the same $[Pt_3(CO)_6]_5^{2-}$ cluster on $\gamma\text{-}Al_2O_3$, but it was not observed on MgO [11]. The behavior of the $[Pt_3(CO)_6]_5^{2-}$ cluster seems to be greatly dependent on the support, as discussed later. The complete disappearance of b-CO was not observed at 348 K. When the temperature was increased to 373 K the desorption of b-CO terminated in 5 min. Further evacuation at 373 K caused the successive desorption of t-CO, as shown in fig. 2. A part of t-CO was not completely removed even after evacuation at 423 K: the evacuation at 423 K for 120 min resulted in the same spectrum as that of fig. 2 (e). It is noticed that the band of t-CO after desorption of b-CO (figs. 1 (i) and 2 (a)) showed a tailing feature to the lower frequency side. The band at 2045 cm^{-1} in fig. 2 (a) was deconvoluted, using a Gaussian function, into two bands: one centered at 2045 cm^{-1} (FWHM = 36 cm^{-1}) and the other at 2023 cm^{-1} (FWHM = 80 cm^{-1}). The appearance of two bands for the species in fig. 2 (a) indicates the existence of two types of t-CO in different environments, and the t-CO observed in fig. 2 (e) is represented by the band deconvoluted to 2035 cm^{-1}. Namely, there are two types of Pt atoms that can adsorb CO: (1) Pt atoms which are not in direct contact with the silica surface and (2) Pt atoms which are in contact with the SiO_2 support. The first type of Pt atoms produce a sharp, intense CO feature at 2045 cm^{-1} and desorption of CO from them

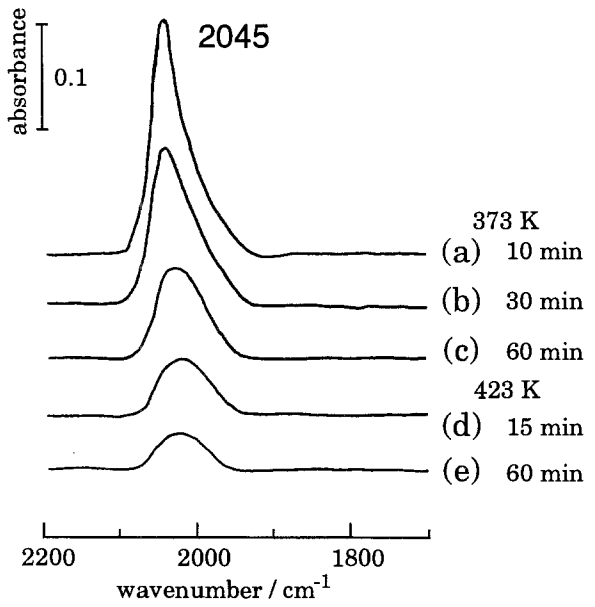

Fig. 2. Thermal treatment of $[Pt_3(CO)_6]_5$ on SiO_2 at 373 K (a–c), and 423 K (d, e). Spectra were measured at 10 min (a), 30 min (b) and 60 min (c) after the temperature of the sample was raised to 373 K; and at 15 min (d), and 60 min (e) after the temperature of the sample was raised to 423 K.

occurs at lower temperature. The Pt atoms in direct contact with the SiO_2 support are electronically and geometrically perturbed by the support, and the adsorbed CO shows a broad band at lower frequency.

The integrated absorbance of bands of the t-CO during evacuation with increasing temperature (figs. 1 and 2) is plotted in fig. 3. The integrated absorbance stayed constant at 298 K, and a monotonous decrease was observed after 10 min at 373 K and at 423 K. This decrease indicates the desorption of t-CO above 373 K on the assumption that the absorption coefficient is unchanged at 373 and 423 K. On the other hand, the integrated absorbance of t-CO slightly increased in the time course at 348 K probably due to the change in absorption coefficient between the original and the interconverted t-CO bands by desorption of b-CO, as mentioned above. It is noted that the amount of t-CO remained unchanged at 348 K and during the first 10 min at 373 K after termination of the absorbance increase, assuming that the absorption coefficient is constant for the same species. This feature implies that thermal desorption of the t-CO occurred after the b-CO completely disappeared, and that the species observed in figs. 1 (i) and 2 (a) could be regarded as $[Pt_3(t\text{-}CO)_3]_5$ or $Pt_{15}(t\text{-}CO)_{15}$, where b-CO is absent. The difference of the two expressions is whether the initial structure of the Pt cluster is maintained (for $[Pt_3(t\text{-}CO)_3]_5$) or reconstructed (for $Pt_{15}(t\text{-}CO)_{15}$).

In order to confirm the structure of Pt_{15} species after the disappearance of b-CO species, the observed IR frequency of t-CO species is discussed by comparison with those adsorbed on Pt single crystal surfaces [16,17] and on supported Pt particles [18–27]. The adsorption site and IR frequency of CO were correlated by studying CO adsorption on a series of Pt particles with different particle sizes supported on SiO_2 and by comparing with those on various surfaces of a Pt single crystal [21–23]. Several peaks of t-CO were observed, and the ratio of peak intensities of their bands were found to differ from one another on changing the particle size as follows [21]. The high frequency band at 2081 cm^{-1} was observed for larger Pt particles, and was assigned to CO adsorbed on the terrace facets with high coordination number [21,22]. The medium frequency band appeared at 2070 cm^{-1} very intensely for the smaller particles ($\sim$ 24 Å diameter) [21]. The low frequency band at 2060 cm^{-1} was found to appear for Pt particles with diameter bigger than 14 Å and increased in intensity on increasing the particle size [21–23]. Then the intensity of the low frequency band gradually decreased on increasing the Pt particle diameter above 15 Å [21]. All the wavenumbers above are referred from ref. [21] presented as singleton frequencies without any dipole–dipole interaction. They shift to higher frequency in the presence of dipole–dipole interaction. The medium and low frequency bands were supposed to be attributable to CO adsorbed on corner and edge sites, respectively [21]. However, on stepped single crystal surfaces, any clear difference was not found

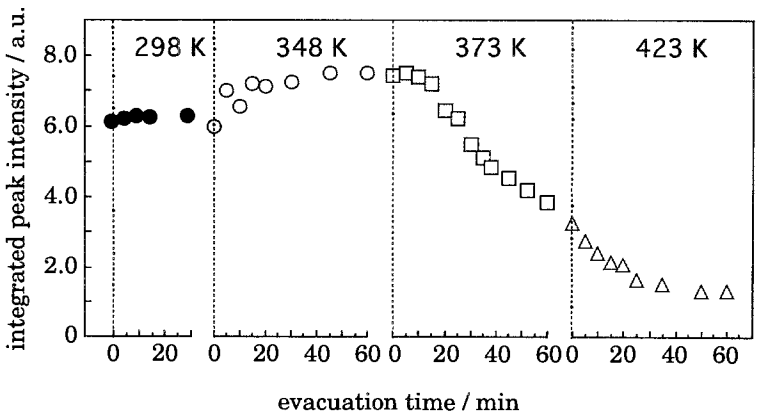

Fig. 3. Change in integrated peak intensity of t-CO with time of thermal treatment between 298 and 423 K.

between CO on corner and edge sites; only a single band at 2065 cm^{-1} (at initial coverage) was observed and clear assignments of adsorption sites of CO on corner and edge sites were not made [21]. In the present study, the band at 2045 cm^{-1} observed at high CO concentration is represented as ~ 2040 cm^{-1} by taking the dipole–dipole interaction into account. The observed peak position of the species in fig. 2 (a) is still low to be ascribed as those at corner or edge sites of SiO_2-supported Pt particles. On the other hand, there are some reports on the frequency of CO adsorbed on SiO_2-supported Pt showing the band at such low frequency as 2045 cm^{-1} [26,27]. It was reported that adsorption of CO at room temperature showed a band at 2062–2079 cm^{-1} and gradual heating (~ 623 K) under evacuation caused a downward shift to 2040 cm^{-1} [26,27]. A hysteresis in coverage–frequency plot was observed and was interpreted as a transformation of the adsorption site from terrace to step ones [26,27]. This confirms us to assign the band at 2045 and 2023 cm^{-1} in fig. 2 (a) to $[Pt_3(t\text{-}CO)_3]_5$ where the initial structure of the cluster is maintained. Consequently, all the CO adsorbed on corner Pt atoms, and those t-CO adsorbed on Pt atoms free from interaction with the support gave a sharp band at 2047 cm^{-1} and those on the SiO_2-interacted Pt atoms at 2023 cm^{-1}.

The change in frequency of the t-CO band after desorption of b-CO at 373 and 423 K is plotted in fig. 4 as a function of integrated peak intensity of t-CO. A linear correlation between the coverage and the frequency was observed at initial decrease of t-CO species, which indicates the occurrence of dipole–dipole interaction for the t-CO appearing at higher frequency. For the low-frequency t-CO remaining at higher temperature, a clear change in frequency on decreasing the amount was not observed because of its broad band shape or of the absence of dipole–dipole interaction. Dipole–dipole interaction was not observed for the t-CO on step sites of SiO_2-supported Pt [26,27] although the IR band was observed at the same frequency as in the present study. This is probably due to small concentration of the step sites on the catalyst: the large distance between the adsorbates prohibited the interaction. In the present study, the observation of the dipole–dipole interaction for the t-CO species at 2045 cm^{-1} supports the concentrated localization of the species, where the five t-CO species protrude to the same direction. The direction corresponds to the vacuum since these t-CO exist on Pt without perturbation by adsorption. Therefore, the $[Pt_3(t\text{-}CO)_3]_5$ clusters are considered to lay on their sides on the support with 5 and 10 Pt atoms with and without interaction with the SiO_2 support. The structure of the Pt cluster which gave the spectrum in fig. 2 (e) is here formally referred to as $Pt_{15}(t\text{-}CO)_n$ ($n \ll 15$) assuming that aggregation did not occur.

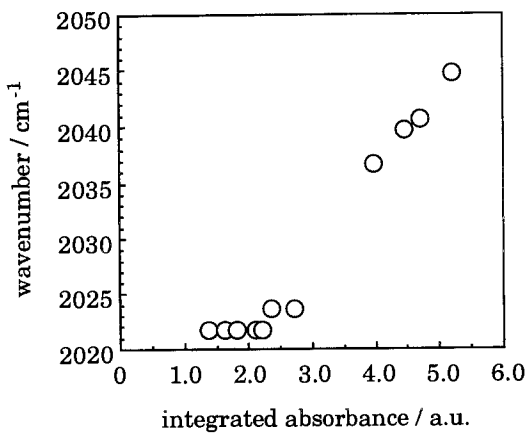

Fig. 4. Relation between the frequency and the integrated peak intensity of t-CO.

3.2. Recarbonylation of $[Pt_3(t\text{-}CO)_3]_5$ species at 298 K

Recarbonylation of $[Pt_3(t\text{-}CO)_3]_5$ species was conducted by introduction of 400 Torr of CO at 298 K, as seen on the IR spectra shown in fig. 5. The band of t-CO shifted from 2047 to 2066 cm^{-1} and a small amount of b-CO was regenerated by the introduction of CO. By evacuation of gas phase CO, the 2066 cm^{-1} band shifted to a lower frequency region accompanied by desorption of some b-CO. These behaviors are the same as those observed during thermal treatment of the original $[Pt_3(t\text{-}CO)_3(b\text{-}CO)_3]_5$, and the spectrum in fig. 5 (d) is identical to that in fig. 1 (h). This species is regarded as $[Pt_3(t\text{-}CO)_3]_5(b\text{-}CO)_n$ ($n < 15$), where the b-CO was incomplete in the original cluster. Complete recarbonylation was not observed on SiO_2 as on γ-Al_2O_3 [10] and MgO [11]. This is perhaps hindered by the strong interaction of some Pt atoms with the support surface formed on desorption of b-CO. The structural change of the cluster from rod-like to hemispherical shape was observed on

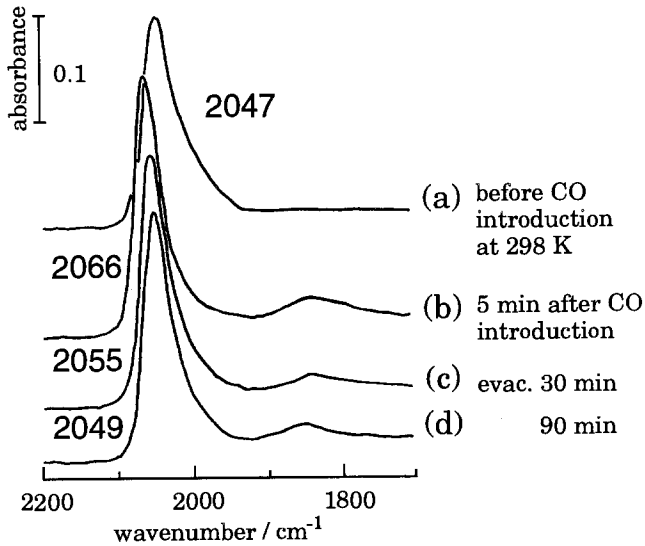

Fig. 5. Recarbonylation of $[Pt_3(t\text{-}CO)_3]_5$ species at 298 K; (a) before carbonylation, (b) after contact with CO for 5 min, (c) after evacuation of gas phase for 30 min, and (d) for 90 min.

MgO after recarbonylation at room temperature [11]. In the present case, however, almost complete regeneration of the partially recarbonylated $[Pt_3(t\text{-}CO)_3]_5(b\text{-}CO)_n$ ($n < 15$) species was observed, as evidenced by the peak transformation from 2047 to 2066 cm^{-1} due to regeneration of b-CO species. Therefore, the Pt skeleton of $[Pt_3(t\text{-}CO)_3]_5$ species is confirmed as maintaining the original structure. The structural transformation is rather considered to take place during decarbonylation of t-CO than upon recarbonylation of $[Pt_3(t\text{-}CO)_3]_5$ species.

3.3. Recarbonylation of $Pt_{15}(t\text{-}CO)_n$ ($n \ll 15$) species at 298 K

Recarbonylation of the $Pt_{15}(t\text{-}CO)_n$ ($n \ll 15$) species (fig. 2 (e)) mentioned in section 3.1 was attempted at 298 K in the same manner as that of the $[Pt_3(t\text{-}CO)_3]_5$ species. The t-CO on the recarbonylated $Pt_{15}(t\text{-}CO)_n$ ($n \ll 15$) gave the band at 2073 cm^{-1}, as observed in fig. 6 (a). The fact that this IR band appeared at higher frequency than ever observed implies that the structural change was derived from the desorption of t-CO species at 423 K, which resulted in a weaker adsorption of t-CO than the original ones. The integrated absorbance also changed, becoming much less than that of the $[Pt_3(t\text{-}CO)_3]_5$ species. It is possible to consider that the amount of adsorbed t-CO decreased due to the aggregation to larger clusters and that the formally inscribed $Pt_{15}(t\text{-}CO)_n$

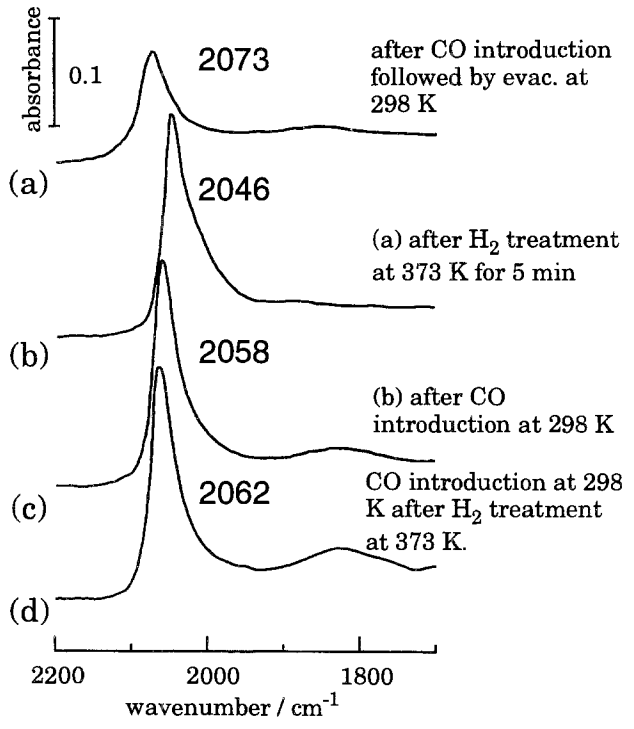

Fig. 6. Recarbonylation of $Pt_{15}(t\text{-}CO)_n$ ($n \ll 15$) species at 298 K; (a) after evacuation of gas phase CO at 298 K, (b) after H_2 treatment of (a), (c) recarbonylation of (b), and (d) recarbonylation of $Pt_{15}(t\text{-}CO)_n$ ($n \ll 15$) species after H_2 treatment.

($n \ll 15$) species was not in its form. However, when the species observed in fig. 6 (a) was treated by 100 Torr of H_2 at 373 K, the spectrum changed to that shown in fig. 6 (b), which is identical to that of $[Pt_3(t\text{-}CO)_3]_5$ (see fig. 5 (a)). It was thus found that the structure of recarbonylated $Pt_{15}(t\text{-}CO)_n$ ($n \ll 15$) species was reformed to $[Pt_3(t\text{-}CO)_3]_5$ species by H_2 treatment, and that the cause of the intensity decrease of t-CO should not be attributed to aggregation but to a decrease in absorption coefficiency. The origin of the decrease in absorption coefficiency to about 46% as well as that of the 27 cm^{-1} blueshift is not clear in the present study. This fact supports that the number of Pt atoms in formally defined $Pt_{15}(t\text{-}CO)_n$ ($n \ll 15$) both before and after recarbonylation stayed at 15, i.e., the Pt_{15} cluster did not aggregate. Therefore, the structure of $Pt_{15}(t\text{-}CO)_n$ ($n \ll 15$) was confirmed and the recarbonylated species before H_2 treatment is regarded as $Pt_{15}(t\text{-}CO)_{15}$, where the number of the t-CO recovered to 15. The b-CO is evidently absent in spectrum (b), since there in no excess CO present that can produce this species. Further adsorption of CO to $[Pt_3(t\text{-}CO)_3]_5$ species (fig. 6 (b)) at 298 K gave a spectrum as shown in fig. 6 (c). A small amount of regeneration of b-CO and an upward frequency shift were observed. The feature by comparison with the recarbonylation of the original $[Pt(t\text{-}CO)_3]_5$ species in fig. 5 indicates that the species in fig. 6 (c) is represented as $[Pt_3(t\text{-}CO)_3]_5(b\text{-}CO)_n$ ($n < 15$) species. The direct H_2 treatment of $Pt_{15}(t\text{-}CO)_n$ ($n \ll 15$) species prior to recarbonylation resulted in the same species $Pt_{15}(t\text{-}CO)_{15}$ as observed in fig. 6 (d). In this case, t- and b-CO were produced simultaneously. Although the clear structure of $Pt_{15}(t\text{-}CO)_n$ or $Pt_{15}(t\text{-}CO)_{15}$ cannot be suggested from the present study, the capability of the Pt_{15} cluster for 15 t-CO species indicates that such form involving any bulk Pt atoms inside the cluster is unlikely and that the reconstruction is not much extensive. Consequently, the original stucture is regenerated by H_2 treatment, however, details of the restructuring process are not clear. The scheme of thermal desorption, recarbonylation and H_2 treatment is summarized in scheme 1, and the possibility of aggregation is excluded.

3.4. Thermal treatment at 573 K

When the sample was evacuated at 573 K, complete decarbonylation took place. Recarbonylation of the completely decarbonylated Pt sample gave the spectrum shown in fig. 7 (a). It is seen that formation of b-CO was totally prohibited and that the line shape of the band is much narrower than the bands ever observed. This indicates that the morphology of the Pt cluster changed from $[Pt_3(t\text{-}CO)_3]_5$ or $Pt_{15}(t\text{-}CO)_n$ ($n \ll 15$) after the complete decarbonylation at 573 K. From the frequency (2066 cm^{-1} at full coverage), the t-CO is assigned to those adsorbed on steps or kinks of larger Pt particles or those of Pt(111) surface [21,23] as mentioned in section 3.1.

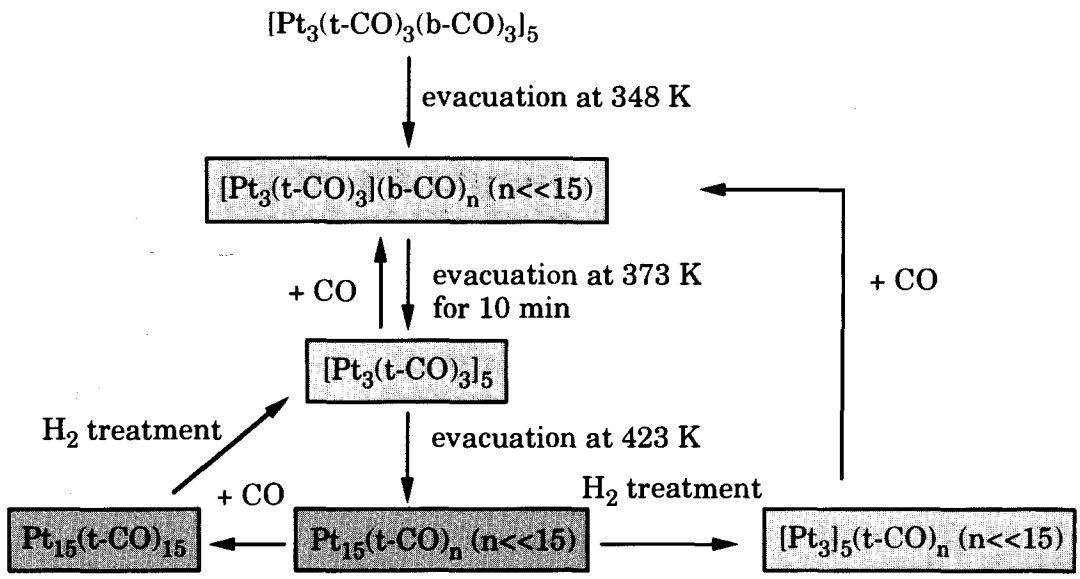

Scheme 1. Proposed reaction schemes of carbonylation and decarbonylation of $[Pt_3(CO)_6]_5$ supported on SiO_2.

The same H_2 treatment as performed for $Pt_{15}(t\text{-}CO)_n$ ($n \ll 15$) was also conducted to this species and gave an apparently different IR spectrum (fig. 7 (b)): regeneration of the $[Pt_3(t\text{-}CO)_3]_5$ species was not observed in this case. The band shifted to a higher frequency region, on the contrary, and decreased in intensity. The redshift is unlikely due to H-coadsorption, since it is reported to cause decrease in CO stretching frequency [28]. This would rather be also a kind of H_2-induced structure transformation and confirms that the irreversible change of the Pt cluster took place at 573 K. In order to look into the b-CO formation, H_2 treatment at 573 K was performed before exposure to CO at 298 K. The resulting spectrum is shown in fig. 7 (c). No b-CO was formed, which supports the great diversity in the structure of the Pt cluster. Once the sample was treated with H_2 at 573 K, there was not any considerable frequency shift of regenerated t-CO after additional H_2 treatment at 373 K (fig. 7 (d)). However, desorption of ca. 15% of CO occurred by the H_2 treatment as seen from the change of fig. 7 (c) to (d), on the basis of equal absorption coefficient, although the same H_2 treatment did not cause any desorption when P_{15} was maintained.

The time course of desorption of t-CO from various species under evacuation at 423 K is plotted in fig. 8. All the samples were evacuated at 298 K after exposure to

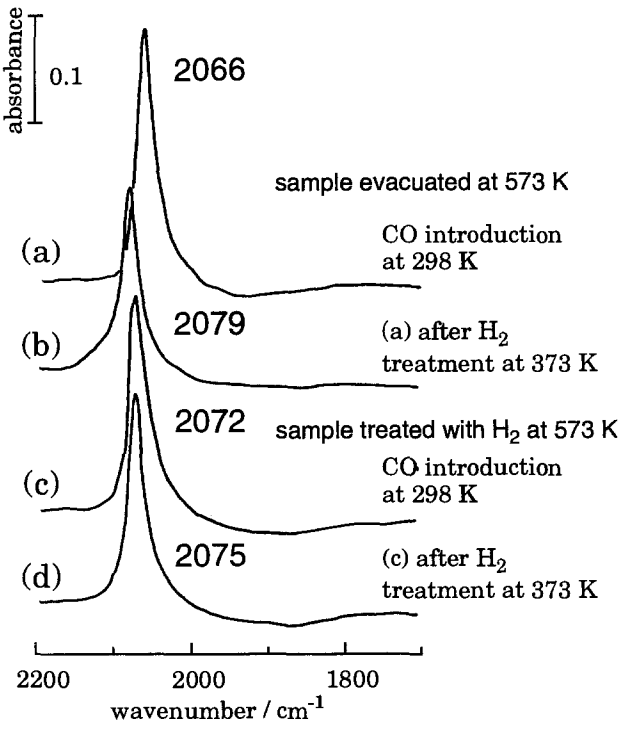

Fig. 7. Recarbonylation of Pt cluster at 298 K after thermal treatment at 573 K; (a) after recarbonylation, (b) after H_2 treatment of (a), (c) recarbonylation after H_2 treatment of the Pt cluster at 573 K, and (d) after H_2 treatment of (c) at 373 K.

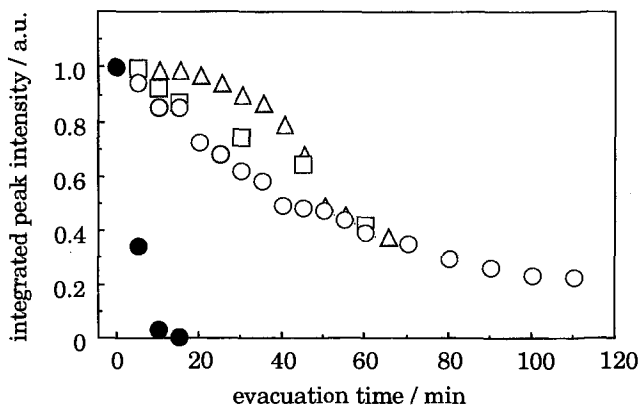

Fig. 8. Time course of integrated peak intensities t-CO in various Pt clusters during evacuation at 423 K; (○) $[Pt_3(t\text{-}CO)_3]_5$ species in fig. 5 (d), (□) $[Pt_3(t\text{-}CO)_3]_5$ species in fig. 6 (d), (△) $Pt_{15}(t\text{-}CO)_{15}$ species in fig. 6 (a), and (●) Pt cluster in fig. 7 (d).

CO, and the temperature was increased to 423 K. The integrated absorbance was normalized by the initial amount, the absorbance observed soon after the temperature reached 423 K. The open circles and the squares correspond to the $[Pt_3(t\text{-}CO)_3]_5$ species in figs. 5 (d) and 6 (d), and the triangles to the $Pt_{15}(t\text{-}CO)_{15}$ species in fig. 6 (a). The gradual release of t-CO was observed for the three samples, and t-CO were not removed completely at the temperature. On the other hand, the t-CO in the cluster represented by the spectrum shown in fig. 7 (d) showed rapid desorption, which completed within 15 min of t-CO. Therefore, the treatment at 573 K is considered to cause aggregation of the Pt_{15} clusters, while the number of the Pt atoms in a cluster presumably stays 15 after thermal treatment below 423 K.

4. Summary

The decarbonylation of $[Pt_3(CO)_6]_5$ grafted on dehydrated SiO_2 was found to produce $[Pt_3(t\text{-}CO)_3]_5$ species by evacuation at 373 K for 10 min. Two different types of t-CO were identified by IR spectra and were assigned to t-CO on Pt atoms in different environment; with and without interaction with the support. The complete decarbonylation was not observed even at 423 K to leave some t-CO in $Pt_{15}(t\text{-}CO)_n$ ($n \ll 15$) form but was observed at 473 K to result in the aggregation of the Pt cluster. The complete recarbonylation of either $[Pt_3(t\text{-}CO)_3]_5$ or $Pt_{15}(t\text{-}CO)_n$ ($n \ll 15$) to the original $[Pt_3(t\text{-}CO)_3(b\text{-}CO)_3]_5$ was not observed and was regarded as due to the interaction of some Pt atoms with the SiO_2 surface.

References

[1] B.C. Gates, L. Guczi and H. Knözinger, eds., *Metal Clusters in Catalysis* (Elsevier, Amsterdam, 1986).
[2] Y. Iwasawa and D. del Rei, eds., *Tailored Metal Catalysis* (Boston, 1986).
[3] J.M. Basset, J.P. Candy, A. Chopin, C. Sanyinic and A. Theolier, Catal. Today 5 (1989) 1.
[4] R. Barth, B.C. Gates, Y. Zhao, H. Knözinger and J. Hulse, J. Catal. 82 (1983) 147.
[5] J. Robertson and G. Web, Proc. Roy. Soc. A 341 (1974) 383.
[6] A.K. Smith, F. Hugues, A. Theolier, J.M. Basset, R. Ugo, G.M. Zanderighi, J.L. Bilhou, V. Bilhou-Boubnol and W.F. Glaydon, Inorg. Chem. 18 (1979) 3104.
[7] S.D. Maloney, F.B.M. Van Zon, M.J. Kelley, D.C. Koningsberger and B.C. Gates, Catal. Lett. 5 (1990) 161.
[8] M. Ichikawa, Chem. Lett. (1976) 335.
[9] J. Bénard, ed., *Adsorption on Metal Surfaces*, Studies in Surface Science and Catalysis, Vol. 13 (Elsevier, Amsterdam, 1983).
[10] B.E. Handy, J.A. Dumesic and S.H. Langer, J. Catal. 126 (1990) 73.
[11] J.-R. Chang, D.C. Koningsberger and B.C. Gates, J. Am. Chem. Soc. 114 (1992) 6460.
[12] G. Li, T. Fujimoto, A. Fukuoka and M. Ichikawa, Catal. Lett. 12 (1992) 171.
[13] J.C. Calabrese, L.F. Dahl, P. Chini, G. Longoni and S. Martinengo, J. Am. Chem. Soc. 96 (1974) 2614.
[14] G. Longoni and P. Chini, J. Am. Chem. Soc. 98 (1976) 7225.
[15] R. Ryberg, *Infrared Spectroscopy of Molecules Adsorbed on Metal Surfaces*, Adv. Chem. Phys., Vol. LXXVI, ed. K.P. Lawley (Wiley, Chichester, 1989).
[16] J.C. Campuzano, in: *Chemisorption Systems*, Part A, The Chemical Physics of Solid Surfaces and Heterogeneous Catalysis, Vol. 3, eds. D.A. King and D.P. Woodruff (Elsevier, Amsterdam, 1990).
[17] P. Hollins and J. Pritchard, *Infrared Studies of Chemisorbed Layers on Single Crystals*, Progress in Surface Science, Vol. 19 (1985) p. 275.
[18] R.P. Eischens, S.A. Francis and W.A. Pliskin, J. Chem. Phys. 60 (1956) 194.
[19] N.W. Cant and R.A. Donaldson, J. Catal. 71 (1981) 320.
[20] N.W. Cant and R.A. Donaldson, J. Catal. 78 (1982) 461.
[21] R.G. Greenler, K.D. Burch, K. Kretzschmar, R. Klauser, A.M. Bradshaw and B.E. Hayden, Surf. Sci. 152/153 (1985) 338.
[22] R.K. Brandt, M.R. Hughes, L.P. Burget, K. Truszkowska and R.J. Greenler, Surf. Sci. 286 (1993) 15.
[23] C. de La Cruz and N. Sheppard, Spectrochim. Acta 50A (1994) 271.
[24] S.D. Jackson, J. Willis, G.D. McLellan, G. Webb, R.B. Moyes, S. Simpson, P.B. Wells and R. Whyman, J. Catal. 139 (1993) 191.
[25] S.D. Jackson, B.M. Glanville, J. Willis, G.D. McLellan, G. Webb, R.B. Moyes, S. Simpson, P.B. Wells and R. Whyman, J. Catal. 139 (1993) 207.
[26] M. Batók, J. Sárkány and A. Sitkei, J. Catal. 72 (1981) 236.
[27] J. Sárkány and M. Batók, J. Catal. 92 (1985) 388.
[28] D. Hoge, M. Tüshaus, E. Schweizer and A.M. Bradshaw, Chem. Phys. Lett. 151 (1988) 230.